

Oxygen Permeability and Stability of $\text{Sr}_{0.95}\text{Co}_{0.8}\text{Fe}_{0.2}\text{O}_{3-\delta}$ in a CO_2 - and H_2O -Containing Atmosphere

Jianxin Yi, Shaojie Feng, Yanbo Zuo, Wei Liu, and Chusheng Chen*

Laboratory of Advanced Functional Materials and Devices, Department of Materials Science and Engineering, University of Science and Technology of China, Hefei, Anhui 230026, People's Republic of China

Received July 26, 2005

The oxygen permeability and stability of a perovskite oxide membrane of nominal composition $\text{Sr}_{0.95}\text{Co}_{0.8}\text{Fe}_{0.2}\text{O}_{3-\delta}$ were investigated in an atmosphere containing CO_2 and H_2O . It was observed that, at a temperature of 810 °C, the oxygen permeation flux through the membrane decreased significantly with time when an air stream containing both CO_2 and H_2O impurities was used as the feed gas and the membrane partially decomposed, whereas in air containing either CO_2 or H_2O species alone, the oxygen flux decreased slightly and the membrane retained its phase composition and microstructure. It was also found that, at a higher temperature of 900 °C, the oxygen flux was almost unaffected by the presence of these species and the membrane remained intact. The effects of CO_2 and H_2O were explained in terms of formation of bicarbonate on the membrane surface, and optimal operation conditions for the membrane were proposed.

1. Introduction

In recent years, oxygen-permeable dense ceramic membranes have received great interest owing to their potential applications in separation of oxygen from air and partial oxidation of methane.^{1–6} The highest oxygen permeability has been reported for perovskite system $\text{La}_{1-x}\text{Sr}_x\text{Co}_{1-y}\text{Fe}_y\text{O}_{3-\delta}$, especially the composition $\text{SrCo}_{0.8}\text{Fe}_{0.2}\text{O}_{3-\delta}$.^{2–4}

For practical applications, the membrane is required to possess high oxygen permeability and sufficient chemical stability. Since most membrane compositions contain basic alkaline-earth elements and rare-earth elements, the membrane tends to react with CO_2 and H_2O in the atmosphere. Degradation of the membranes in the presence of CO_2 and H_2O has been reported.^{7–9} Benson et al. studied the structural degradation of $\text{La}_{0.6}\text{Sr}_{0.4}\text{Fe}_{0.8}\text{Co}_{0.2}\text{O}_{3-\delta}$ in CO_2 and H_2O atmospheres.⁷ Carolan et al. reported that the oxygen permeation flux at 783 °C through perovskite $\text{La}_{0.2}\text{Ba}_{0.8}\text{Co}_{0.8}\text{Fe}_{0.2}\text{O}_{3-\delta}$ decreased with time in CO_2 -containing air and further decreased when H_2O was added.⁸ Similar

degradation was also observed for many other oxide materials such as proton conductor doped BaCeO_3 , superconductor $\text{YBa}_2\text{Cu}_3\text{O}_{7-\delta}$, and oxygen sensor Mg-doped SrTiO_3 .^{10–14}

Moreover, it has been known for some time that the chemical stability of the ABO_3 perovskite oxide is related to its cation stoichiometry. For example, A-site-deficient $\text{La}_{0.2}\text{Sr}_{0.8}\text{Co}_{0.41}\text{Fe}_{0.41}\text{Cu}_{0.2}\text{O}_{3-\delta}$ possesses a greater resistance against the corrosion of CO_2 and H_2O than $\text{La}_{0.2}\text{Sr}_{0.79}\text{Co}_{0.39}\text{Fe}_{0.31}\text{Cu}_{0.27}\text{O}_{3-\delta}$ with an A-site excess,¹⁵ and A-site-deficient Sr-doped LaMnO_3 , a widely used cathode material for solid oxide fuel cells, exhibited less reactivity toward the yttria-stabilized zirconia electrolyte in comparison with that of stoichiometric composition.^{16,17}

In the present work, a perovskite oxide membrane of composition $\text{Sr}_{0.95}\text{Co}_{0.8}\text{Fe}_{0.2}\text{O}_{3-\delta}$ was investigated in terms of its oxygen permeability and chemical stability in the presence of CO_2 and H_2O . Its strontium content was chosen to be less than unity for stability consideration of the membrane.

2. Experimental Section

A sample of nominal composition $\text{Sr}_{0.95}\text{Co}_{0.8}\text{Fe}_{0.2}\text{O}_{3-\delta}$ (denoted SCF95) was synthesized via a solid-state reaction route. Appropriate

* To whom correspondence should be addressed. Phone: +86-551-3602940. Fax: +86-551-3601592. E-mail: ccsn@ustc.edu.cn.

- (1) Chen, C. S.; Feng, S. J.; Ran, S.; Zhu, D. C.; Liu, W.; Bouwmeester, H. J. M. *Angew. Chem., Int. Ed.* **2003**, *42*, 5196.
- (2) Teraoka, Y.; Zhang, H. M.; Furukawa, S.; Yamazoe, N. *Chem. Lett.* **1985**, 1743.
- (3) Kruidhof, H.; Bouwmeester, H. J. M.; v. Doorn, R. H. E.; Burggraaf, A. J. *Solid State Ionics* **1993**, *63–65*, 816.
- (4) Qiu, L.; Lee, T. H.; Liu, L. M.; Yang, Y. L.; Jacobson, A. J. *Solid State Ionics* **1995**, *76*, 321.
- (5) Dyer, P. N.; Richards, R. E.; Russek, S. L.; Taylor, D. M. *Solid State Ionics* **2000**, *134*, 21.
- (6) Griffin, T.; Sundkvist, S. G.; Åsen, K.; Bruun, T. *J. Eng. Gas Turbines Power* **2005**, *127*, 81.
- (7) Benson, S. J.; Waller, D.; Kilner, J. A. *J. Electrochem. Soc.* **1999**, *146*, 1305.
- (8) Carolan, M. F.; Dyer, P. N.; LaBar, J. M., Sr.; Thorogood, R. M. U.S. Patent 5,240,473, 1993.
- (9) Shao, Z. P.; Yang, W. S.; Cong, Y.; Dong, H.; Tong, J. H.; Xiong, G. X. *J. Membr. Sci.* **2000**, *172*, 177.

- (10) Ryu, K. H.; Haile, S. M. *Solid State Ionics* **1999**, *125*, 355.
- (11) Günther, W.; Schöllhorn, R.; Siegle, H.; Thomsen, C. *Solid State Ionics* **1996**, *84*, 23.
- (12) Borowiec, K.; Przyluski, J.; Kolbrecka, K. *J. Am. Ceram. Soc.* **1991**, *74*, 2007.
- (13) Zheng, H.; Sørensen, O. T.; Liu, X. Q.; Jensen, H. *J. Electroceram.* **1999**, *3*, 301.
- (14) Zheng, H.; Sørensen, O. T. *J. Eur. Ceram. Soc.* **1999**, *19*, 1987.
- (15) Carolan, M. F.; Dyer, P. N.; Motika, S. A.; Alba, P. B. U.S. Patent 5,712,220, 1998.
- (16) Jiang, S. P.; Zhang, J. P.; Ramprakash, Y.; Milosevic, D.; Wilshier, K. *J. Mater. Sci.* **2000**, *35*, 2735.
- (17) Østergård, M. J. L.; Clausen, C.; Bagger, C.; Mogensen, M. *Electrochim. Acta* **1995**, *40*, 1971.

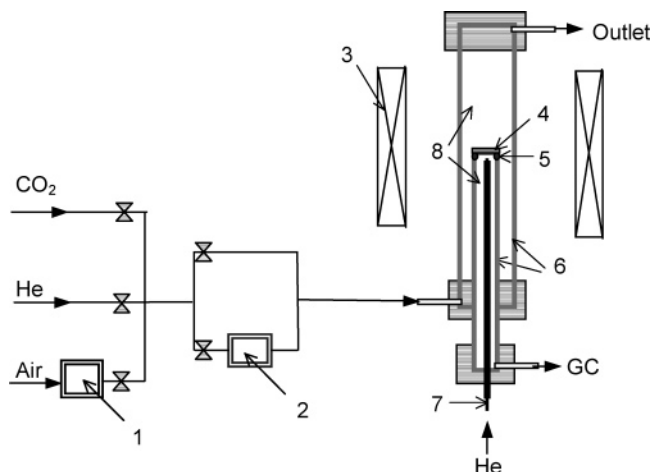


Figure 1. Experimental setup for oxygen permeation measurements: (1) 5A molecular sieves, (2) water bath, (3) furnace, (4) sample, (5) glass sealant, (6) alumina tube, (7) thermocouple, (8) oxygen permeation cell.

amounts of SrCO₃ (AR), Fe₂O₃ (AR), and Co₂O₃ (AR) were mixed and ball-milled. The obtained mixture was calcined in air at 950, 1050, and 1100 °C for 10 h with intermittent grinding by ball-milling. The calcined powder was isostatically pressed into pellets at 300 MPa, and then sintered at 1150 °C in air for 10 h. The densities of the sintered pellets were measured to be ~94% of the theoretical density by means of the Archimedes method using mercury.

Some of the SCF95 powder and sintered pellet samples were annealed for 24 h at temperatures of 810 and 900 °C in a controlled gas air stream containing CO₂ and H₂O and then quenched in the ambient atmosphere. The volume fraction of H₂O was set at 4 vol % by passing an air stream through a water bath maintained at 30 °C, and that of CO₂ in the air stream was fixed at 5 vol %. The air used was prepurified by 5A molecular sieves.

The phase composition of the samples was analyzed by XRD (Philips X'Pert Pro Super, Cu Kα). The surface composition of the sintered sample was measured by XPS (ESCALAB MK II, VG). The microstructure was observed by SEM (Hitachi X-650 and JEOL JSM-6700F) coupled with INCA energy-dispersive X-ray spectroscopy (EDX).

The chemical composition of the samples was analyzed by titration and inductively coupled plasma (ICP) emission spectroscopy (Atomscan Advantage). Therein, HCl and HNO₃ aqueous solutions of the sample were prepared for titration and ICP analysis, respectively. The details of chemical titration can be found elsewhere.¹⁸

Isothermal gravimetric analysis was carried out in a home-built apparatus equipped with an analytical balance to investigate the reaction of the material with CO₂ and H₂O. A 1.7–2.0 g sample of SCF95 powder was placed in a quartz sample holder suspended from the balance with a hooked quartz stick. When the sample weight reached a constant in a helium-balanced air stream, a CO₂-and/or H₂O-containing air stream was introduced and the weight change was monitored.

Oxygen permeation measurements were performed using the apparatus shown in Figure 1. Disk-shaped membranes of thickness 1.50–1.70 mm were sealed to an alumina tube by a glass ring sealant at 1000 °C and then cooled to measurement temperatures. One side of the membrane was exposed to a flowing air stream, while the other side was swept with a highly pure helium stream to remove the permeated oxygen. Both the O₂ and N₂ concentrations

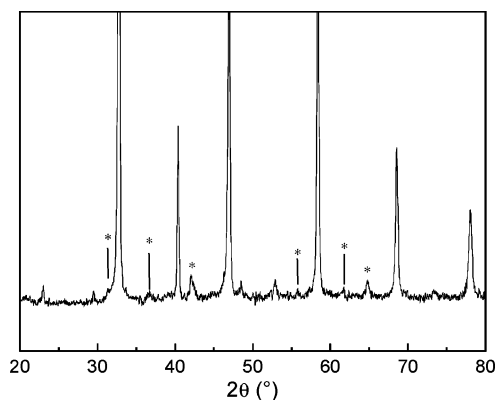


Figure 2. XRD pattern of an as-prepared SCF95 sample: (*) cobalt/iron oxides.

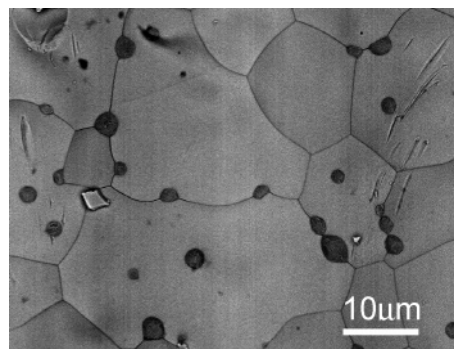


Figure 3. Backscattered electron image of an SCF95 pellet.

in the permeated effluent gas stream were analyzed by a gas chromatograph (GC9750).

3. Results

3.1. Phase and Chemical Composition. Figure 2 presents the X-ray diffraction patterns for the as-prepared sample. The main peaks can be assigned to a cubic perovskite phase which is similar to SrCo_{0.81}Fe_{0.19}O_{2.78} (JCPDS 82-2445), and the weak diffraction peaks at $2\theta = 31.3^\circ, 36.6^\circ, 42.1^\circ, 55.7^\circ, 61.7^\circ,$ and 64.8° can be attributed to cobalt/iron oxides such as (Co,Fe)O and (Co,Fe)₃O₄. Figure 3 shows the backscattered electron image of a fresh sintered SCF95 pellet. Some small black particles are located at the grain boundaries and within the large grains. EDX analysis revealed that the large grains correspond to the perovskite phase and the small grains to cobalt/iron oxides.

Figure 4 gives the strontium 3d_{3/2}–d_{5/2} XPS spectrum for a fresh sintered SCF95 pellet. The spectrum consists of two doublets. The first doublet is at binding energies of 131.4 and 133.2 eV and the second at 133.7 and 135.5 eV. The first doublet is assigned to bulk strontium and the second to surface strontium.¹⁹ Their contributions to the total Sr 3d spectrum are 37% and 63%, respectively, revealing that the surface is enriched with strontium.

The chemical composition for the as-prepared sample was also measured. The Co/Fe ratio was determined by titration and ICP to be 4.1 and 4.0, respectively. The values are very close to the nominal one of 4.0. The Sr/(Co + Fe) ratio

(18) Zheng, C. H. M.Sc. Thesis, University of Science and Technology of China, 2003.

(19) van Doorn, R. H. E.; Bouwmeester, H. J. M.; Burggraaf, A. J. *Solid State Ionics* **1998**, *111*, 263.

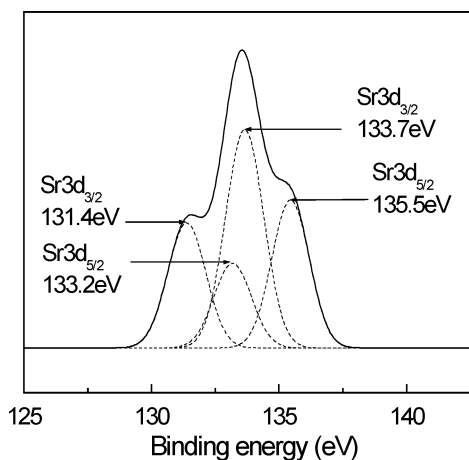


Figure 4. Sr 3d_{3/2}-d_{5/2} XPS spectrum for the fresh surface of an SCF95 pellet.

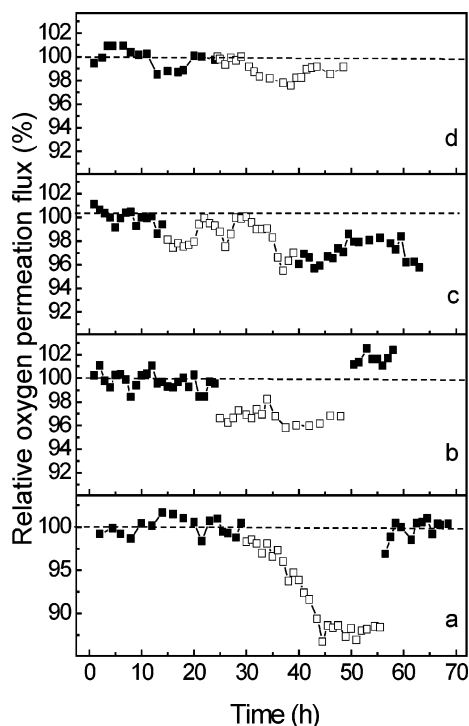


Figure 5. Oxygen permeation behavior of SCF95 membranes using different feed gases and at various temperatures: (a) air containing both 4 vol % H₂O and 5 vol % CO₂, 810 °C; (b) air containing 5 vol % CO₂ alone, 810 °C; (c) air containing 4 vol % H₂O alone, 810 °C; (d) air containing both 4 vol % H₂O and 5 vol % CO₂, 900 °C; (■) helium-balanced air; (□) air containing CO₂ and/or H₂O. Dashed lines are guides to the eye.

measured by both methods was 0.98, higher than the nominal value of 0.95. (The relative errors were about 0.5% and 1% for titration and ICP, respectively.) In preparing the solutions for chemical titration and ICP analysis, some small particles were found insoluble in HCl or HNO₃ aqueous solution. These particles were determined by XRD to be (Co,Fe)₃O₄, which may account for the discrepancy in the Sr/(Co + Fe) ratio between the measured and the nominal values.

3.2. Oxygen Permeability. Figure 5 shows the oxygen permeation behavior of SCF95 membranes on exposure to various atmospheres containing CO₂ and/or H₂O, in which the oxygen permeation fluxes were scaled by the steady oxygen fluxes measured using a helium-balanced air as the feed gas.

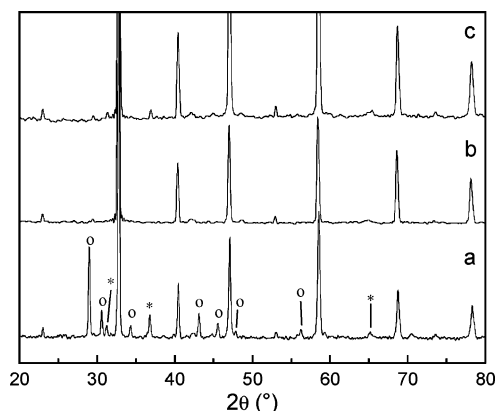


Figure 6. XRD patterns of the feed side surface of SCF95 pellets after permeation at 810 °C using air containing (a) both H₂O and CO₂, (b) CO₂ alone, and (c) H₂O alone as the feed gas: (*) (Co,Fe)₃O₄; (O) unknown phase.

At 810 °C, when an air stream containing both 5 vol % CO₂ and 4 vol % H₂O was introduced as the feed gas, the oxygen flux decreased gradually with time in the first 13 h and then remained almost constant in the following 13 h, yielding a drop of ~12% from 1.21 to 1.07 (mL/cm²)/min in the flux; however, the flux recovered rapidly after the air stream was switched back to a 9 vol % helium-balanced one. When an air stream containing 5 vol % CO₂ alone was used, the oxygen flux decreased quickly by ~3% and then remained almost unchanged afterward; the flux could also be recovered to the original value after replacement of CO₂ in the feed air with 5 vol % helium. When an air stream containing 4 vol % H₂O alone was introduced, the oxygen flux fluctuated with time, and a decrease of about 3% resulted 24 h after introduction of the humid air, but the flux could not be recovered after the air stream was switched back to dried air balanced with 4 vol % helium. Clearly, the decrease in the oxygen permeation flux in the presence of both CO₂ and H₂O at 810 °C is much larger than that in the presence of either CO₂ or H₂O species alone.

It was found that the effect of CO₂ and H₂O impurities on the oxygen permeability was less severe at higher temperatures. When the temperature was raised to 900 °C, as shown in Figure 5d, the oxygen flux was hardly affected by CO₂ and H₂O. This is consistent with the observation by Carolan et al., who found that the oxygen permeation flux through La_{0.2}Ba_{0.8}Co_{0.8}Fe_{0.2}O_{3-δ} decreased at 783 °C but remained constant at 837 °C in an atmosphere containing CO₂ and H₂O.⁸

3.3. Chemical Stability. Figure 6 shows the XRD patterns obtained from the feed side surface of the membrane samples after oxygen permeation measurement at 810 °C. For membranes permeated in an air stream containing both CO₂ and H₂O, some extra diffraction peaks appeared (Figure 6a). These peaks cannot be assigned to either carbonates or hydrates, suggesting formation of an unknown phase and partial decomposition of the perovskite phase. However, for membranes permeated in an air stream containing either CO₂ or H₂O species alone, the phase composition remained almost unchanged (Figure 6b,c). It is worthwhile to note that, for membranes permeated at a higher temperature of 900 °C, the phase composition as revealed by XRD was not affected

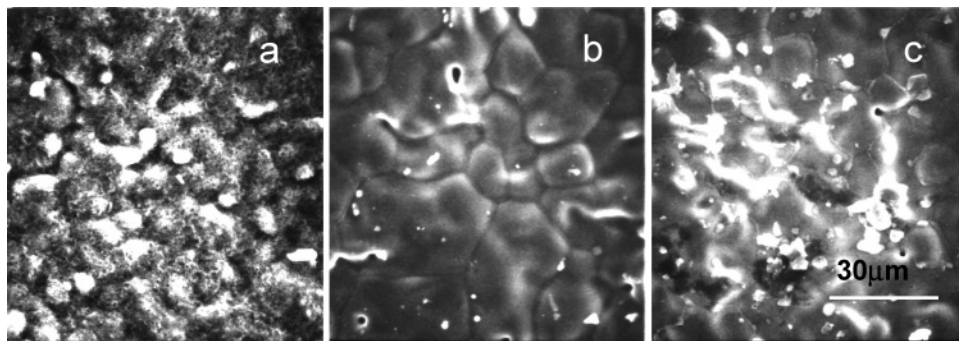


Figure 7. Feed side surface morphologies of SCF95 pellets after permeation at 810 °C using air containing (a) both H₂O and CO₂, (b) CO₂ alone, and (c) H₂O alone as the feed gas.

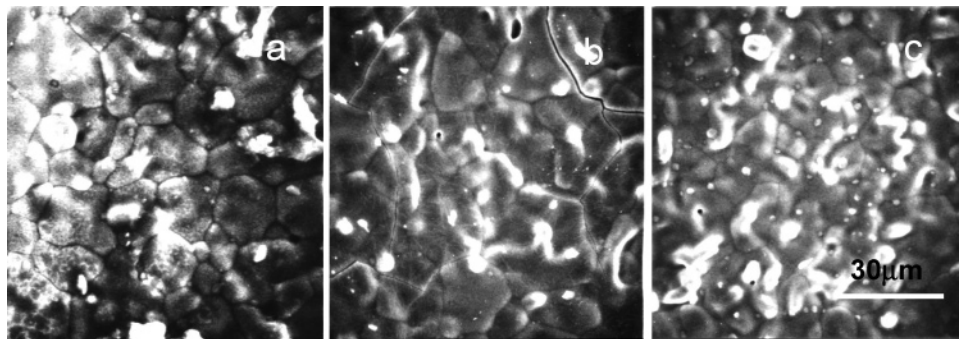


Figure 8. SEM pictures of SCF95 pellets annealed at 810 °C in air containing (a) both CO₂ and H₂O, (b) CO₂ alone, and (c) H₂O alone.

by the presence of both CO₂ and H₂O, in contrast to that of the membrane permeated at 810 °C. Figure 7 gives the SEM pictures for the feed side surface of the membranes permeated at 810 °C. For the membrane permeated in the air stream containing both CO₂ and H₂O, the morphology changed to a large extent; especially, the surface became rather porous (Figure 7a). However, for the membrane permeated in the air stream containing CO₂ alone, the microstructure remained almost unchanged (Figure 7b). As for the membrane permeated in the air stream containing H₂O alone, electrical charging was observed at the grain boundaries on the feed side surface of the membrane during SEM observation (Figure 7c); this reveals that the grain boundaries were less conductive in comparison with the interior grains, suggesting that the grain boundaries were preferentially attacked by H₂O during oxygen permeation.

For a better understanding of the influence of the CO₂ and H₂O impurities on the membrane, sintered pellets were annealed in various atmospheres at a temperature of 810 °C and compared with the permeated membranes. Unlike the permeated membranes, no change in phase composition was detected by XRD on the annealed samples. However, some changes in the microstructures were observed with SEM (Figure 8), although the extent of the changes was much less than that for the permeated membranes. To manifest the effects of CO₂ and H₂O impurities, powder samples were also examined, since the powder samples possessed a much larger surface area than the sintered dense pellets. For the powder annealed in air containing both CO₂ and H₂O at 810 °C, an unknown phase appeared as evidenced by two weak diffraction peaks at $2\theta = 28.7^\circ$ and 44.1° (Figure 9a). To identify which species, CO₂ or H₂O, is responsible for the occurrence of this unknown phase, powder samples were

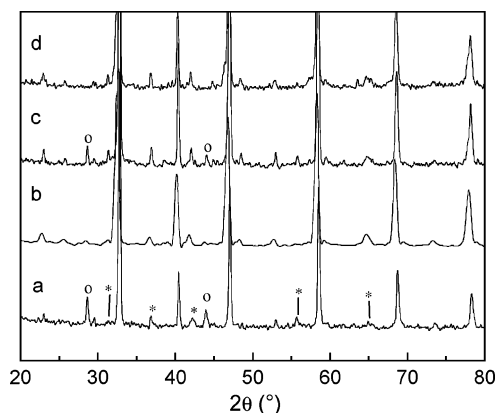


Figure 9. X-ray diffraction patterns of annealed SCF95 powders: (a) at 810 °C in air containing both CO₂ and H₂O; (b) at 810 °C in air containing CO₂ alone; (c) at 810 °C in air containing H₂O alone; (d) powder obtained in (c) reannealed at 900 °C in air; (*) cobalt/iron oxides; (O) unknown phase.

annealed in air containing either CO₂ or H₂O species alone. It turned out that the unknown phase appeared in the sample annealed in air containing H₂O alone, but not in the sample annealed in air containing CO₂ alone (Figure 9b,c). This suggests that it is H₂O rather than CO₂ that plays a dominant role in the degradation of the membrane under the given conditions. The other important observations from the annealing experiments are that, when the temperature was raised to 900 °C, the phase composition was not altered by the contained CO₂ and H₂O and annealing at 900 °C could even eliminate the unknown phase that had been formed during annealing at a lower temperature of 810 °C (Figure 9d).

The effects of CO₂ and H₂O impurities in the air were also examined by isothermal gravimetry. As shown in Figure 10a, when an air stream containing both 5 vol % CO₂ and 4

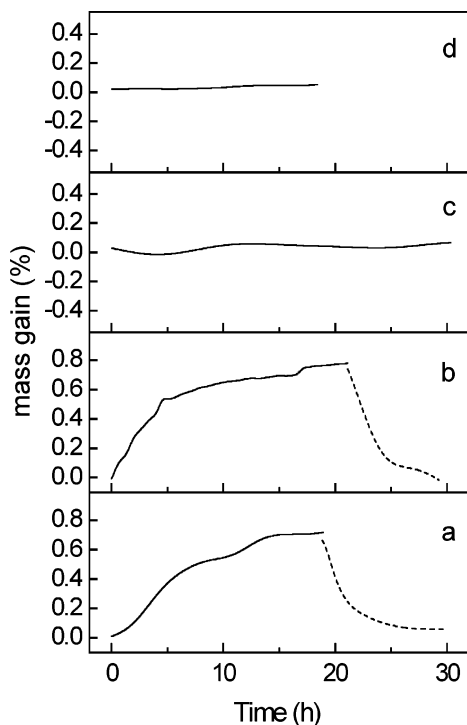


Figure 10. Weight changes of SCF95 powders in different atmospheres and at various temperatures: (a) air containing both H₂O and CO₂, 810 °C; (b) air containing CO₂ alone, 810 °C; (c) air containing H₂O alone, 810 °C; (d) air containing both H₂O and CO₂, 900 °C. Solid and dashed lines denote the introduction and removal of CO₂ and/or H₂O gas impurities, respectively.

vol % H₂O was introduced at 810 °C, the weight of the powder sample increased with time, resulting in an increment of about 0.72% in a time period of 19 h; the powder was quickly restored to the original weight upon removal of CO₂ and H₂O. When 5 vol % CO₂ alone was introduced, a weight gain of 0.76% was observed after 19 h (Figure 10b). However, the presence of 4 vol % H₂O alone in the air did not cause any weight change within the experimental errors (Figure 10c). It is also worthwhile to note that the weight gain caused by the incorporation of CO₂ became insignificant when the temperature was raised to 900 °C (Figure 10d).

4. Discussion

It is revealed by the present study that the phase composition, surface morphology, and oxygen permeability of the SCF95 membrane are adversely affected by the copresence of CO₂ and H₂O species in the feed air, compared with the presence of either species alone. These effects are more pronounced when an oxygen partial pressure gradient is applied and the membrane is operated at lower temperatures.

Both theoretical and experimental studies have indicated that a H₂O–CO₂ van der Waals complex is formed when both CO₂ and H₂O are present in the gas phase.^{20,21} This complex can react on TiO₂ oxide surfaces to form bicarbonate,^{22,23} and the oxygen vacancies on the oxide surface are suggested to play an essential role in the formation of

bicarbonate.²⁴ Bicarbonate is also likely to form on the surfaces of the Sr_{0.95}Co_{0.8}Fe_{0.2}O_{3-δ} membrane, which contains a large concentration of oxygen vacancies. The formation of the bicarbonate is accompanied by the decomposition of the membrane and thus a decrease in oxygen permeability. This study shows that, in comparison with the membrane exposed to both CO₂ and H₂O species, the membrane exposed to either species alone is less affected, which may be simply due to the absence of the bicarbonate whose formation would require the presence of both species. Moreover, this study shows that the permeated membrane degrades to a large extent, in comparison with the annealed membrane. Note that an oxygen gradient is applied to the former membrane but not to the latter. Therefore, one may speculate that the formation of the bicarbonate is enhanced by the applied oxygen gradient. This study also shows that the effect of CO₂ and H₂O on the membrane is severe at a lower temperature of 810 °C but at a higher temperature of 900 °C it is almost negligible. This may be explained as follows. The formation reaction of bicarbonate is associated with a decrease in entropy; thus, it is not favored by an increase in temperature.

In light of practical application of a perovskite oxygen-permeable membrane, the copresence of CO₂ and H₂O should be avoided due to the joint effect of these two species. In comparison with CO₂, H₂O is easier to remove from the feed air by cold condensation. This approach is also justified by the present study, which shows that CO₂ is less harmful to the membrane than H₂O under the given experimental conditions. Although CO₂ is incorporated into the membrane to a larger extent, it does not cause a significant change to the microstructure and phase composition. In contrast, although H₂O is not incorporated into the membrane obviously, it brings about changes in the phase composition and microstructure of the membrane, resulting in an irreversible decrease of the oxygen permeability. The other approach of reducing or even eliminating the adverse effect of CO₂ and H₂O is to operate the membrane at higher temperatures.

The present study centers on the effect of a small amount of CO₂ and H₂O in the feed air, but for a number of proposed applications, the membrane is required to operate under much higher partial pressures of CO₂ and H₂O.^{5,6} For example, in a proposed advanced zero emissions power plant integrating the membrane-based oxygen separation and methane combustion units,⁶ the permeate side of the membrane is swept with the exhaust gas stream from the combustion unit. Since the sweeping gas contains concentrated CO₂ and H₂O, great challenges are imposed on the membrane. Therefore, the study of the effects of CO₂ and H₂O on the performance of the membrane must be extended to these stringent operation conditions.

5. Conclusions

The copresence of CO₂ and H₂O species in air has severe effects on the phase composition, microstructure, and oxygen

(20) Merz, K. M. *J. Am. Chem. Soc.* **1990**, *112*, 7973.

(21) Peterson, K. I.; Klemperer, W. J. *Chem. Phys.* **1984**, *80*, 2439.

(22) Primet, M.; Pichat, P.; Mathieu, M. V. *J. Phys. Chem.* **1971**, *75*, 1221.

(23) Tanaka, K.; White, J. M. *J. Phys. Chem.* **1982**, *86*, 4708.

(24) Henderson, M. A. *Surf. Sci.* **1998**, *400*, 203.

permeability of a Sr_{0.95}Co_{0.8}Fe_{0.2}O_{3-δ} membrane, compared with the presence of either species alone. The presence of an oxygen partial pressure gradient and use of lower operation temperatures enhance the degradation of the membrane. The adverse effects of CO₂ and H₂O species may be related to the formation of bicarbonate on the membrane surface, and an increase in the operation temperature and

removal of either CO₂ or H₂O species from the feed air can improve the membrane performance.

Acknowledgment. This work was supported by the National Science Foundation of China (Grant Nos. 50225208 and 50332040).

CM051636Y